

# Cold Dark Matter Substructure and Galactic Disks

Stelios Kazantzidis<sup>1</sup>, Andrew R. Zentner<sup>2</sup>, and James S. Bullock<sup>3</sup>

<sup>1</sup>Center for Cosmology and Astro-Particle Physics, The Ohio State University,  
 191 West Woodruff Avenue, Columbus, OH 43210, USA  
 email: [stelios@mps.ohio-state.edu](mailto:stelios@mps.ohio-state.edu)

<sup>2</sup>Department of Physics & Astronomy, University of Pittsburgh,  
 100 Allen Hall, 3941 O'Hara Street, Pittsburgh, PA 15260, USA  
 email: [zentner@pitt.edu](mailto:zentner@pitt.edu)

<sup>3</sup>Center for Cosmology, Department of Physics & Astronomy,  
 The University of California at Irvine, 4168 Reines Hall, Irvine, CA 92697, USA  
 email: [bullock@uci.edu](mailto:bullock@uci.edu)

## Abstract.

We perform a set of high-resolution, fully self-consistent dissipationless  $N$ -body simulations to investigate the influence of cold dark matter (CDM) substructure on the dynamical evolution of thin galactic disks. Our method combines cosmological simulations of galaxy-sized CDM halos to derive the properties of substructure populations and controlled numerical experiments of consecutive subhalo impacts onto initially-thin, fully-formed disk galaxies. We demonstrate that close encounters between massive subhalos and galactic disks since  $z \sim 1$  should be common occurrences in  $\Lambda$ CDM models. In contrast, extremely few satellites in present-day CDM halos are likely to have a significant impact on the disk structure. One typical host halo merger history is used to seed controlled  $N$ -body experiments of subhalo-disk encounters. As a result of these accretion events, the disk thickens considerably at all radii with the disk scale height increasing in excess of a factor of 2 in the solar neighborhood. We show that interactions with the subhalo population produce a wealth of distinctive morphological signatures in the disk stars, many of which resemble those being discovered in the Milky Way (MW), M31, and in other disk galaxies, including: conspicuous flares; bars; low-lived, ring-like features in the outskirts; and low-density, filamentary structures above the disk plane. We compare a resulting dynamically-cold, ring-like feature in our simulations to the Monoceros ring stellar structure in the MW. The comparison shows quantitative agreement in both spatial distribution and kinematics, suggesting that such observed complex stellar components may arise naturally as disk stars are excited by encounters with subhalos. These findings highlight the significant role of CDM substructure in setting the structure of disk galaxies and driving galaxy evolution.

**Keywords.** cosmology: theory, dark matter, galaxies: formation, galaxies: dynamics, galaxies: structure, methods: numerical

---

## 1. Introduction

The currently favored cold dark matter (CDM) paradigm of hierarchical structure formation (e.g., Blumenthal et al. 1984), predicts significant dark matter halo substructure in the form of small, dense, self-bound *subhalos* orbiting within the virialized regions of larger host halos (e.g., Klypin et al. 1999). Observational probes of substructure abundance thus constitute fundamental tests of the CDM model. Due to the fact that most subhalos associated with galaxy-sized host halos lack of a significant luminous component, a constraint on the amount of substructure in these systems may be obtained via their gravitational influence on galactic disks. If there is a considerable subhalo popula-

tion, it may produce strong tidal effects and induce distinctive gravitational signatures which might be imprinted on the structure and kinematics of the host galactic disk. Thus, establishing the role of substructure in shaping the fine structure of galactic disks may prove fundamental in informing our ideas about global properties of galaxy formation and evolution.

Significant theoretical effort has been devoted to quantifying the resilience of galactic disks to infalling satellites (e.g., Quinn & Goodman 1986; Velazquez & White 1999; Font et al. 2001; Gauthier et al. 2006; Read et al. 2008; Villalobos & Helmi 2008). Despite their usefulness, most earlier investigations suffered basic shortcomings that limited their applicability. For example, some considered encounters of single satellites with galactic disks, a set-up which is at odds with CDM predictions of multiple, nearly contemporaneous accretion events. Other studies made ad hoc assumptions about the orbital parameters and internal structures of the infalling systems. Consequently, it remains uncertain whether these earlier investigations faithfully captured the responses of galactic disks to halo substructure in a cosmological context.

Here we address this issue using a hybrid approach that combines cosmological simulations to derive the merger histories of galaxy-sized CDM halos with controlled numerical experiments of consecutive subhalo impacts onto  $N$ -body realizations of fully-formed disk galaxies. We demonstrate that accretion histories of the kind expected in  $\Lambda$ CDM models are capable of severely perturbing galactic disks and generating a wealth of distinctive signatures in the structural and kinematic properties of disk stars. The resulting morphological features are similar to those being discovered in the Milky Way (MW), M31, and in other disk galaxies. We also show that satellite-disk interactions produce dynamically-cold, ring-like features around galactic disks that are quantitatively similar to the Monoceros ring in the MW. This suggests that such observed stellar structures may arise naturally as a result of subhalo-disk encounters, which can excite perturbations in *disk stars*. These findings imply that detailed observations of galactic structure may be able to distinguish between competing cosmological models by determining whether the detailed structure of galactic disks is as excited as predicted by the CDM paradigm.

## 2. Methods

The aim of this study is to assess the effects of CDM substructure on the dynamical evolution of thin galactic disks. A thorough description of our methods is presented in Kazantzidis et al. (2007) and we summarize them here. First, we analyze cosmological simulations of the formation of four galaxy-sized halos in the  $\Lambda$ CDM cosmology. The simulations were performed with the Adaptive Refinement Tree (ART)  $N$ -body code (Kravtsov 1999). All of these halos accrete only a small fraction of their final masses and experience no major mergers at  $z \lesssim 1$  (a look-back time of  $\approx 8$  Gyr), and therefore may reasonably host a disk galaxy. Second, we identify subhalos in these hosts and select the massive substructures that pass near the center of the host halo where they may interact appreciably with a galactic disk for further consideration. Finally, we use a representative subset of these accretion events from one of the host halos to seed controlled  $N$ -body simulations of satellite impacts onto an initially-thin disk galaxy.

While the present work is informed by many past numerical investigations of satellite-disk interactions, our methodology is characterized by at least three major improvements. First, we consider satellite populations whose properties (mass functions, internal structures, orbital parameters, and accretion times) are extracted directly from the cosmological simulations of galaxy-sized CDM halos. This eliminates many assumptions regarding the internal properties and impact parameters of infalling systems inherent in

many previous studies. Second, we employ primary disk galaxy models that are both self-consistent and flexible enough to permit detailed modeling of actual galaxies such as the MW and M31 by fitting to a wide range of observational data sets (Widrow & Dubinski 2005). This allows us to set up thin, equilibrium realistic disk galaxies without instabilities and transient effects that can be present in other schemes. In this work, we employ galaxy model MWb of Widrow & Dubinski (2005) which reproduces many of the observed characteristics of the MW galaxy. This galaxy model comprises an exponential stellar disk with a  $\text{sech}^2$  scale height of  $z_d = 400$  pc, a Hernquist model bulge, and an NFW dark matter halo.

Lastly, and most importantly, we incorporate for the first time a model in which the infalling subhalo populations are representative of those that impinge upon halo centers since  $z \sim 1$ , instead of the  $z = 0$  surviving substructure present in a CDM halo. Previous studies utilized the *present-day* properties of a large ensemble of dark matter subhalos in order to investigate the dynamical effects of substructure on galactic disks (Font et al. 2001; Gauthier et al. 2006). Successes notwithstanding, this methodology has the drawback of eliminating from consideration those massive satellites that, prior to  $z = 0$ , pass very close to the central regions of their hosts, where the galactic disk resides. These systems can potentially produce strong tidal effects on the disk, but are unlikely to constitute effective perturbers at  $z = 0$  as they suffer substantial mass loss during their orbital evolution precisely because of their forays into the central halo (e.g., Zentner & Bullock 2003).

Figure 1 illustrates the importance of accounting for subhalo infall over time. This figure is a scatter plot of mass versus pericentric distance for two different satellite populations within all four galaxy-sized host CDM halos. The masses and distances in Figure 1 have been scaled to the mass,  $M_{\text{disk}} = 3.53 \times 10^{10} M_{\odot}$ , and radial scale length,  $R_d = 2.82$  kpc, of the stellar disk in the primary galaxy model used in the satellite-disk encounter simulations. For the purposes of this presentation, we have also scaled the virial quantities ( $M_{\text{vir}}$  and  $r_{\text{vir}}$ ) of all four galaxy-sized host halos to a common host of *total* mass,  $M_h = 7.35 \times 10^{11} M_{\odot}$ , and *tidal* radius,  $R_h = 244.5$  kpc, as in the primary disk galaxy model. The dotted line encloses an area in the  $M_{\text{sub}} - r_{\text{peri}}$  plane corresponding to subhalos more massive than  $0.2M_{\text{disk}}$  with pericenters of  $r_{\text{peri}} \lesssim 20$  kpc ( $r_{\text{peri}} \lesssim 7R_d$ ). We refer to this area as the “danger zone”. Satellites within this area are expected to constitute effective perturbers and may cause considerable damage to the disk, but we intend this as a rough criterion to aid in illustrating our point.

The first satellite population in Figure 1 consists of the  $z = 0$  surviving substructures. The second subhalo population consists of systems that approach the central regions of their hosts since a redshift  $z = 1$ . These subhalos cross within a (scaled) infall radius of  $r_{\text{inf}} = 50$  kpc from the host halo center. This selection is fixed empirically to identify orbiting substructure that are likely to have a significant dynamical impact on the structure of the disk (Kazantzidis et al. 2007). The masses associated with this group of satellites are defined at the simulation output time nearest the inward crossing of  $r_{\text{inf}}$ . Pericenters are computed from the orbit of a test particle in a static NFW potential whose properties match those of the host CDM halo at the time of  $r_{\text{inf}}$ .

Figure 1 demonstrates that the  $z = 0$  subhalo populations contain very few massive systems on potentially damaging orbits. In fact, statistics of all four galaxy-sized host halos indicate that only *one* satellite can be identified inside the danger zone in this case. On the other hand, the danger zone contains numerous substructures that passed through or near the galactic disk since  $z = 1$ . On average,  $\sim 5$  satellites more massive than  $0.2M_{\text{disk}}$  cross through the central region of a galaxy-sized halo with  $r_{\text{peri}} \lesssim 20$  kpc during this period. This suggests that close encounters between massive subhalos and galactic

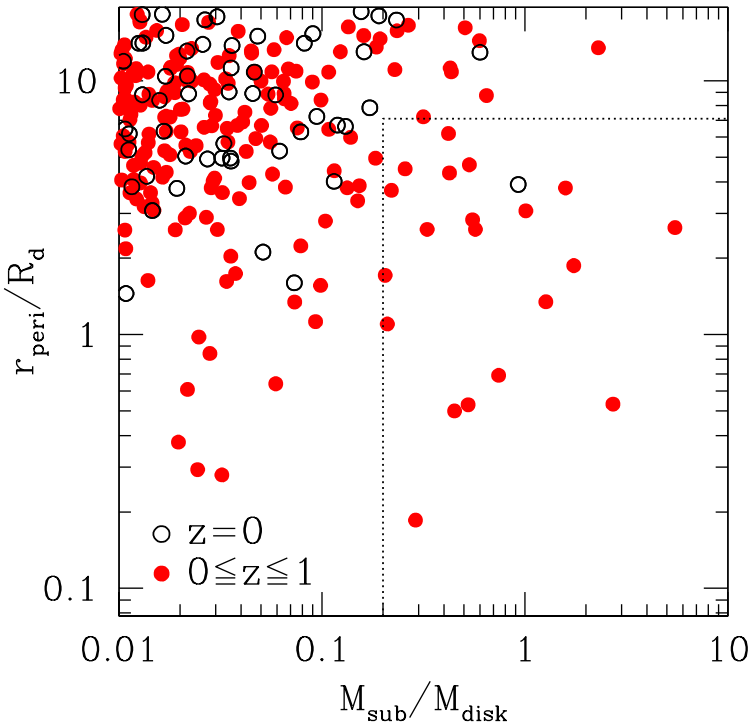


**Figure 1.** A scatter plot of mass versus pericentric distance for satellites identified in four galaxy-sized halos formed in the  $\Lambda$ CDM cosmology. Subhalo masses and orbital radii are presented in units of the mass,  $M_{\text{disk}} = 3.53 \times 10^{10} M_{\odot}$ , and radial scale length,  $R_d = 2.82$  kpc, respectively, of the galactic disk in the controlled simulations. *Filled* symbols show results for subhalos that pass closer than an infall radius of  $r_{\text{inf}} = 50$  kpc of their host halo center since a redshift  $z = 1$ . *Open* symbols refer to the  $z = 0$  population of surviving substructures. *Dotted* lines mark the so-called “danger zone” ( $M_{\text{sub}} \gtrsim 0.2 M_{\text{disk}}$  and  $r_{\text{peri}} \lesssim 20$  kpc) corresponding to infalling subhalos that are likely capable of substantially perturbing the galactic disk. Accretions of massive subhalos onto the central regions of their hosts, where the galactic disk resides, since  $z \sim 1$  should be common occurrences in standard  $\Lambda$ CDM. In contrast, very few satellites in present-day subhalo populations are likely to have a significant dynamical impact on the disk structure.

disks since  $z = 1$  are common occurrences in standard  $\Lambda$ CDM. Thus, it is important to account for such accretion events to model the cumulative dynamical effects of halo substructure on disk galaxies.

In what follows, we focus on one of the host halo accretion histories to seed controlled  $N$ -body experiments of subhalo-disk encounters. We identify target satellites that are likely to have a substantial effect on the disk structure by imposing two selection criteria. First, we limit our search to satellites that approach the central region of their host with small orbital pericenters ( $r_{\text{peri}} \lesssim 20$  kpc) since  $z = 1$ . Second, we restrict re-simulation to subhalos that are a significant fraction of the disk mass, but not more massive than the disk itself ( $0.2 M_{\text{disk}} \lesssim M_{\text{sub}} \lesssim M_{\text{disk}}$ ). The aforementioned criteria resulted in six accretion events of satellites with masses and tidal radii of  $7.4 \times 10^9 \lesssim M_{\text{sub}}/M_{\odot} \lesssim 2 \times 10^{10}$ , and  $r_{\text{tid}} \gtrsim 20$  kpc, respectively, from a single host to simulate over a  $\sim 8$  Gyr period. Additional properties of these substructures can be found in Kazantzidis et al. (2007). We modeled subhalo impacts onto the disk as a sequence of encounters. Starting

with the first satellite, we included subsequent systems at the epoch when they were recorded in the cosmological simulation.

We extracted the density structures of these cosmological subhalos and followed the procedure outlined in Kazantzidis et al. (2004) to construct self-consistent,  $N$ -body realizations of satellites models. Each system was represented with  $N_{\text{sat}} = 10^6$  particles and a gravitational softening length of  $\epsilon_{\text{sat}} = 150$  pc. For the primary disk galaxy, we used  $N_d = 10^6$  particles to represent the disk,  $N_b = 5 \times 10^5$  in the bulge, and  $N_h = 2 \times 10^6$  in the dark matter halo, and softenings of  $\epsilon_d = 50$  pc,  $\epsilon_b = 50$  pc, and  $\epsilon_h = 100$  pc, respectively. All satellite-disk encounter simulations were carried out using PKDGRAV (Stadel 2001).

The “final” disk discussed in the next sections has experienced all six subhalo impacts and was evolved in isolation for  $\sim 4$  Gyr after the last interaction. This ensures that all of the resultant morphological features are long-lived rather than transient. Consequently, our results are relevant to systems that exhibit no obvious, ongoing encounters. Finally, we compute all disk properties and show all visualizations of the disk morphology after centering the disk to its center of mass and rotating it to a new coordinate frame defined by the three principal axes of the total disk inertia tensor.

### 3. Global Disk Morphology

Figure 2 depicts the transformation of the global structure of a thin galactic disk that experiences a merging history of the kind expected in the  $\Lambda$ CDM paradigm of structure formation. This figure shows face-on and edge-on views of the initial and final distribution of disk stars. Particles are color-coded on a logarithmic scale with brighter colors in regions of higher stellar density.

Figure 2 demonstrates that encounters with CDM substructure are responsible for generating several distinctive morphological signatures in the disk. The final disk is considerably thicker (or “flared”) compared to the initial distribution of disk stars and a wealth of low-density features have developed both in and above the disk plane as a consequence of these disturbances. Particularly intriguing is the fact that a high-density, in-plane structure survives after the satellite bombardment. A standard “thin-thick” disk decomposition analysis for the final disk indicates that this feature would be recognized as a thin disk component (Kazantzidis et al. 2007). The edge-on view of the final disk also reveals additional filamentary structures and other complex configurations above the disk plane. These structures bear some resemblance to tidal streams, but are in fact disk stars that have been excited by the subhalo impacts. Interestingly, the same image shows a characteristic “X” shape in the bright central disk, a finding also reported by Gauthier et al. (2006). This feature is often linked to secular evolution of galaxies driven by the presence of a bar when it buckles as a result of becoming unstable to bending modes.

The face-on image of the final disk illustrates the formation of a moderately strong bar and extended ring-like features in the outskirts of the disk. The existence of these features indicate that the axisymmetry of the disk has been destroyed by the encounters with the infalling subhalos. We emphasize that the aforementioned structures are persistent, surviving for a considerable time after the satellite passages ( $\sim 4$  Gyr), and that the bar is induced in response to the accretion events, not by amplified noise. Both features drive further evolution by redistributing mass and angular momentum throughout the disk. Thus, encounters with infalling satellites affect galactic disks both *directly* by imparting energy to stars and *indirectly* by exciting global instabilities. Lastly, the final face-on disk is significantly more structured at low densities and large radii compared to the initial

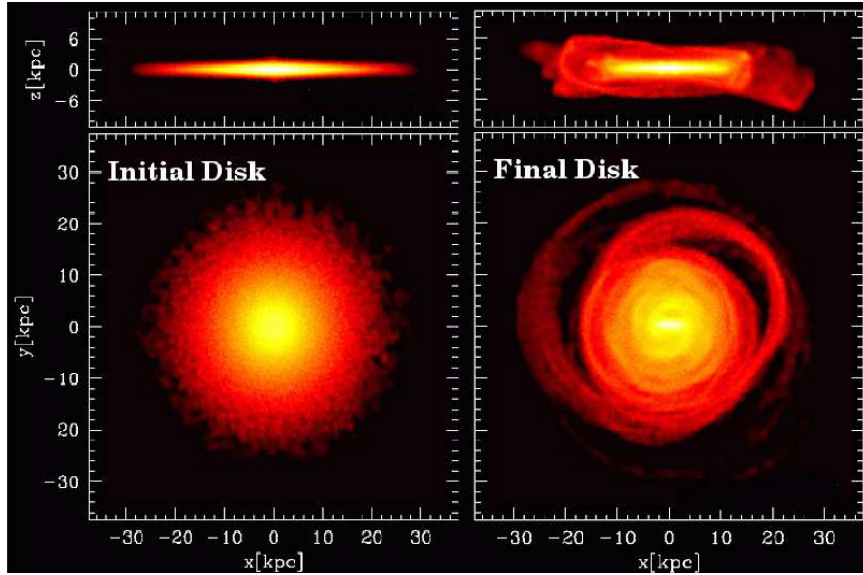


**Figure 2.** Density maps of disk stars illustrating the global morphological transformation of a galactic disk subject to a  $\Lambda$ CDM-motivated satellite accretion history. The *left* panel shows the initial disk assuming that the sequence of satellite-disk interactions initiates at  $z = 1$ , while the *right* panel depicts the disk after the last satellite passage, evolved in isolation for additional  $\sim 4$  Gyr, so that the evolution of disk stars is followed from  $z = 1$  to  $z = 0$ . The edge-on (*upper panels*) and face-on (*bottom panels*) views of the disk are displayed in each frame and the local density was calculated using an SPH smoothing kernel of 32 particles. Satellite-disk interactions of the kind expected in  $\Lambda$ CDM models produce several distinctive signatures in galactic disks including: long-lived, low-surface brightness, ring-like features in the outskirts; conspicuous flares; bars; and faint filamentary structures above the disk plane that (spuriously) resemble tidal streams in configuration space. These morphological features are similar to those being discovered in the Milky Way, M31, and in other disk galaxies.

disk and is quite reminiscent of the outer disk structure seen around M31 (Ibata et al. 2005).

#### 4. Disk Thickening

Among the most striking signatures induced by the subhalo accretion events in our simulations is the pronounced increase in disk thickness. A quantitative analysis of disk thickening is presented in Figure 3. This figure shows that the initial disk thickens considerably at all radii as a result of the substructure impacts. Remarkably, the scale height of the disk near the solar radius increases in excess of a factor of 2. The outer disk is much more susceptible to damage by the infalling satellites: at  $R = R_d$  the scale height grows by  $\sim 50\%$  compared to approximately a factor of 3 increase at  $R = 4R_d$ . The larger binding energy of the inner, exponential disk and the presence of a massive bulge ( $M_b \sim 0.3M_{\text{disk}}$ ) that acts as a sink of satellite orbital energy are responsible for the robustness of the inner disk. Given that infalling subhalos are very extended and the self-gravity of the disk grows weaker as a function of distance from the center, it is not unexpected that the scale height of the disk should increase with radius yielding a flared disk. Indeed, making the simplest assumption that the accreting satellites deposit their orbital energy roughly constant in radius, it can be shown that the disk scale height will

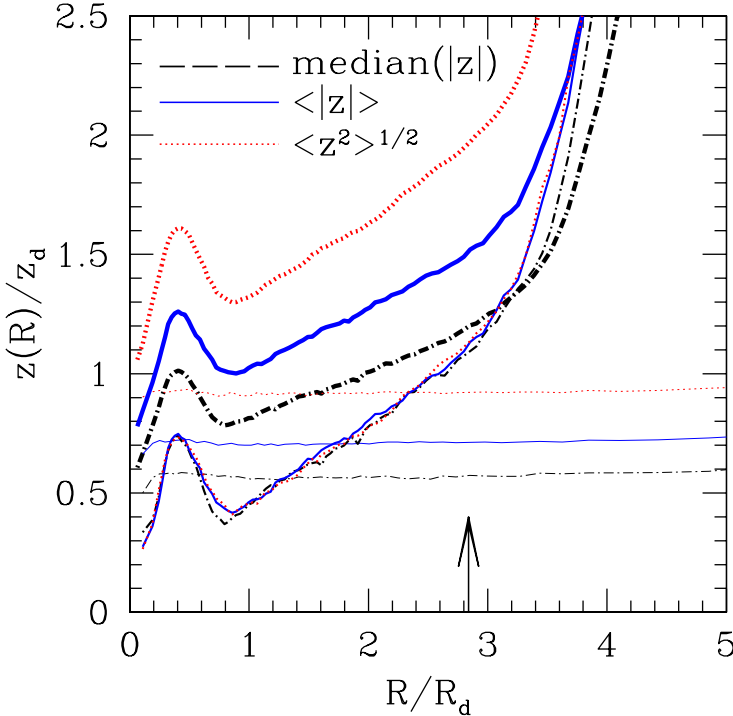


**Figure 3.** Disk thickening. Thickness profiles,  $z(R)$ , for the disk initially (thin lines) and after the satellite passages (thick lines). Lines of intermediate thickness show the fractional increase in disk thickness caused by the subhalo bombardment. Profiles are normalized to the initial disk scale height,  $z_d$ , and are plotted as a function of projected radius in units of the disk radial scale length,  $R_d$ . Different lines correspond to different measures of disk thickness. The arrow indicates the location of the solar radius,  $R_\odot$ . The galactic disk thickens considerably at all radii as a result of the encounters with CDM substructure.

increase as  $\Delta z(R) \propto \Sigma_d^{-2}(R)$ , where  $\Sigma_d(R)$  is the disk surface density (Kazantzidis et al. 2007).

Font et al. (2001) and Gauthier et al. (2006) performed similar numerical studies of the dynamical response of disks to CDM subhalos. Both investigations reported negligible tidal effects on the global structure of the disk. In contrast, Figure 3 indicates substantial disk thickening due to substructure bombardment. The primary reason for this discrepancy is that we followed the formation *history* of a host halo since  $z \sim 1$ , whereas Font et al. (2001) and Gauthier et al. (2006) considered the  $z = 0$  population of surviving substructure present in a CDM halo. As we mentioned above, this difference is critical because as subhalos on highly eccentric orbits at early epochs continuously lose mass, the fraction of massive satellites with small orbital pericenters that are most capable of severely perturbing the disk declines with redshift so that few remain by  $z = 0$ .

## 5. The Monoceros Ring

The face-on view of the final disk in Figure 2 reveals the existence of pronounced ring-like features at its outskirts. These low-density, long-lived dynamically-cold rings are nearly in-plane and are qualitatively similar to the Monoceros ring, an intriguing stellar structure known to extend around the MW (Newberg et al. 2002). This coherent feature spans  $\sim 170^\circ$  degrees around the Galaxy and lies near the disk plane at a Galacto-centric

distance of  $\sim 20$  kpc (e.g., Newberg et al. 2002). It is unclear whether this structure is yet another example of tidal debris from an accreted dwarf galaxy (e.g., Yanny et al. 2003) or a stellar extension of the disk itself (e.g., Ibata et al. 2003).

The reminiscence of the resultant rings in our simulations to that of the Monoceros ring is suggestive that the latter may have been generated via an excitation of an ancient disk's stars. In order to check the general validity of this scenario, Figure 4 presents a direct comparison between the ring-like structures generated via satellite-disk interactions and the Monoceros ring feature towards the Galactic anticenter. The circles in this figure correspond to a kinematic study of M giant stars by Crane et al. (2003), a follow-up to the Rocha-Pinto et al. (2003) effort to identify M giants associated with the ring. We choose the Crane et al. (2003) sample because these data span the Monoceros stream uniformly over  $\sim 100^\circ$  with both precise membership criteria and good velocity determinations. For definiteness, we focus our analysis on the distribution of stars at galacto-centric radii larger than 15 kpc. These stars are color-coded according to their radial position from the center of the disk. Figure 4 shows vertical distance above the disk plane ( $z$ ), heliocentric distance, and heliocentric radial velocity of these stars as a function of Galactic longitude,  $l$ .

It is worth emphasizing that the stars in our simulated data are more finely sampled than those of Crane et al. (2003). To facilitate further comparison, in the lower-right panel, we have more precisely identified a stream-feature along four bins in longitude  $l = [240 - 210, 210 - 180, 180 - 150, 150 - 120]^\circ$  and associated cuts in helio-centric distance  $d_{\text{helio}} = [14 - 12, 12.5 - 10, 12.5 - 10, 12.5 - 10]$  kpc. The four diamonds correspond to the median line-of-sight velocities and longitudes in each of these angular bins. The bars reflect the line-of-sight velocity dispersion in each bin, which is approximately  $\sigma_{\text{los}} \simeq 40 \text{ km s}^{-1}$  across the stream. We stress that using the Crane et al. (2003) data across the first three of these bins we measured a line-of-sight velocity dispersion of  $\sigma_{\text{los}} \simeq 39 \text{ km s}^{-1}$ , consistent with the corresponding values associated with the simulated data. Note that Crane et al. (2003) estimate a line-of-sight velocity dispersion of  $\sigma_{\text{los}} = 20 \pm 4 \text{ km s}^{-1}$  for the ring, which differs significantly from the aforementioned value of  $\sigma_{\text{los}} \simeq 39 \text{ km s}^{-1}$ . This is because the former was calculated using a subset of 53 of the 58 stars in their sample, obtained after a  $2.5\sigma$  ( $\pm 50 \text{ km s}^{-1}$ ) rejection threshold was applied about a third-order polynomial fit to the velocity trend. When we perform a similar rejection threshold within each of our four angular bins we find  $\sigma_{\text{los}} \sim 24.5 \text{ km s}^{-1}$  for our simulated ring, a value consistent with the quoted velocity dispersion for the Monoceros stream from Crane et al. (2003).

The general agreement in the properties of rings generated in our simulations with those of the Monoceros ring structure is encouraging. This agreement is particularly noteworthy because our simulation program did *not* aim to reproduce such a feature. Our simulation campaign has explored only one realization of a galaxy-sized halo accretion history and we tuned no aspect of the computations to produce this agreement. This is a significant point that bears emphasis. One may contrast our model of a disk origin for the Monoceros stream to previous models that have attempted to explain this structure via the accretion and disruption of a satellite galaxy (Peñarrubia et al. 2005). Neither our model nor the model of Peñarrubia et al. (2005) can be falsified by extant data; however, our ring was produced as an unforeseen byproduct of our simulation campaign while the Peñarrubia et al. (2005) ring was produced as part of a program aimed at tuning a satellite accretion event to yield a structure similar to the Monoceros ring. Lastly, it is important to emphasize that accreted-star models seem to require accretion events on nearly-circular, low-inclination orbits. Orbits of this type are quite rare for satellites that penetrate deep into the host halo (e.g., Ghigna et al. 1998). Our disk-excitation scenario

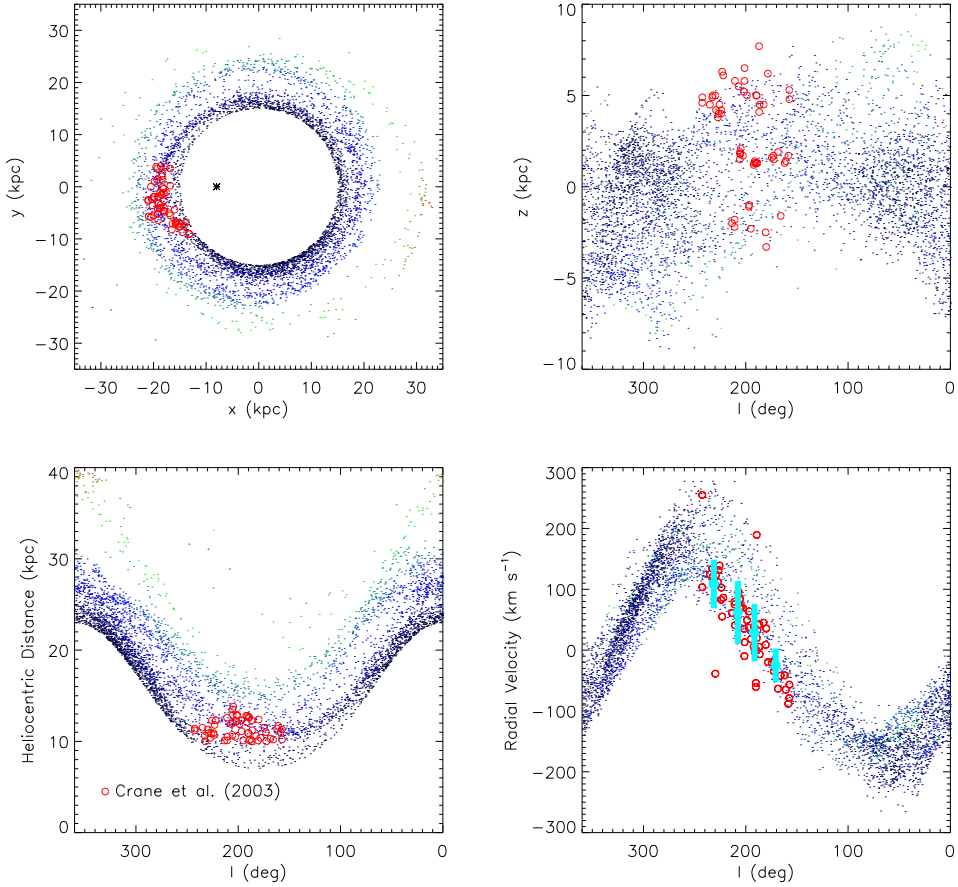


**Figure 4.** Monoceros ring comparison. Circles are data of M giant stars from the Crane et al. (2003) study of the Monoceros stream in the direction of the Galactic anticenter. Points in each panel correspond to stars in the outer regions ( $R > 15$  kpc) of the final disk. These stars are color-coded according to their galacto-centric radius, with dark blue/black at  $R = 15$  kpc, light-blue at  $R \simeq 18$  kpc, green at  $R \simeq 22$  kpc, and orange/red at  $R \gtrsim 25$  kpc. The *upper-left panel* shows a face-on view of the disk and the asterisk marks the adopted position of the Sun at  $(x, y, z) = (8, 0, 0)$  kpc. The *upper-right, lower-left*, and *lower-right* panels show vertical distance of stars above the disk plane,  $z$ , heliocentric distance, and heliocentric radial velocity, respectively, as a function of Galactic longitude in degrees,  $l$ . *Diamonds* in the lower-right panel correspond to the median line-of-sight velocities in four bins in longitude  $l = [240 - 210, 210 - 180, 180 - 150, 150 - 120]^\circ$  for a specific stream-feature identified in the simulations. The associated bars reflect the line-of-sight velocity dispersion in each bin. Accretion histories of the kind expected in  $\Lambda$ CDM models produce dynamically-cold, ring-like features around galactic disks that are quantitatively similar to the Monoceros ring in the MW.

thus constitutes a viable alternative for the origin of the Monoceros ring in the context of  $\Lambda$ CDM.

It is crucial to be able to distinguish between these alternative mechanisms for generating structures such as the Monoceros ring. In principle, the metallicity distribution of stars in the stream can be used to constrain the competing models. The stars in an accreted satellite would generally be expected to have different metallicity from disk stars, while in our model the metallicity of the stream should be comparable to the metallicity

of the thick disk stars surrounding the stream. Unfortunately, metallicity estimates of Monoceros ring stars span a range of values and there is no definitive conclusion that can be reached at present. Similar uncertainties exist for the characterization of the outer thick disk. If the outer thick disk is as metal rich as the canonical thick-disk value,  $[Fe/H] \approx -0.7$  to  $-1$  (Gilmore et al. 1995; Ivezić et al. 2008), the higher ring metallicities estimated by Crane et al. (2003) and Ivezić et al. (2008) would be consistent with our scenario, while the lower ring metallicities reported by Yanny et al. (2003) would be discordant. Overall, the robust utilization of metallicity constraints requires refining the observational measurements for the Monoceros ring and securing the metallicity spread in the outer thick disk. Moreover, precise predictions would require simulations of star formation and metal enrichment.

Another promising method that may falsify a disk-excitation scenario is to identify ring populations that are not expected to pre-exist in the outer disk. Interestingly, there have been indications that some globular clusters may be associated with the Monoceros stream (Crane et al. 2003). While this association is still a matter of debate, the existence of such globular clusters would point to an external origin for the Monoceros structure. Nevertheless, the dynamical study we present is robust and though disk-excitation by substructure may not be the source of the Monoceros feature, low-surface brightness features of this kind should not be uncommon about disk galaxies.

## References

Blumenthal, G. R., Faber, S. M., Primack, J. R., & Rees, M. J. 1984, *Nature*, 311, 517

Crane, J. D., Majewski, S. R., Rocha-Pinto, H. J., Frinchaboy, P. M., Skrutskie, M. F., & Law, D. R. 2003, *Ap. Lett.*, 594, L119

Font, A. S., Navarro, J. F., Stadel, J., & Quinn, T. 2001, *Ap. Lett.*, 563, L1

Gauthier, J.-R., Dubinski, J., & Widrow, L. M. 2006, *ApJ*, 653, 1180

Ghigna, S., Moore, B., Governato, F., Lake, G., Quinn, T., & Stadel, J. 1998, *MNRAS*, 300, 146

Gilmore, G., Wyse, R. F. G., & Jones, J. B. 1995, *AJ*, 109, 1095

Ibata, R., Chapman, S., Ferguson, A. M. N., Lewis, G., Irwin, M., & Tanvir, N. 2005, *ApJ*, 634, 287

Ibata, R. A., Irwin, M. J., Lewis, G. F., Ferguson, A. M. N., & Tanvir, N. 2003, *MNRAS*, 340, L21

Ivezić, Ž. et al. 2008, *ApJ* accepted (astro-ph/0804.3850)

Kazantzidis, S., Bullock, J. S., Zentner, A. R., Kravtsov, A. V., & Moustakas, L. A. 2007, *ApJ* accepted (astro-ph/0708.1949)

Kazantzidis, S., Magorrian, J., & Moore, B. 2004, *ApJ*, 601, 37

Klypin, A., Kravtsov, A. V., Valenzuela, O., & Prada, F. 1999, *ApJ*, 522, 82

Kravtsov, A. V. 1999, PhD thesis, New Mexico State University

Newberg, H. J. et al. 2002, *ApJ*, 569, 245

Peñarrubia, J. et al. 2005, *ApJ*, 626, 128

Quinn, P. J. & Goodman, J. 1986, *ApJ*, 309, 472

Read, J. I., Lake, G., Agertz, O., & Debattista, V. P. 2008, *MNRAS* accepted (astro-ph/0803.2714)

Rocha-Pinto, H. J., Majewski, S. R., Skrutskie, M. F., & Crane, J. D. 2003, *Ap. Lett.*, 594, L115

Stadel, J. G. 2001, Ph.D. Thesis, Univ. of Washington

Velazquez, H. & White, S. D. M. 1999, *MNRAS*, 304, 254

Villalobos, Á. & Helmi, A. 2008, *MNRAS* submitted (astro-ph/0803.2323)

Widrow, L. M. & Dubinski, J. 2005, *ApJ*, 631, 838

Yanny, B. et al. 2003, *ApJ*, 588, 824

Zentner, A. R. & Bullock, J. S. 2003, *ApJ*, 598, 49